Effect of Particle Size on Droplet Infiltration into Hydrophobic Porous Media as a Model of Water Repellent Soil

Christopher A. E. Hamlett[1], Neil J. Shirtcliffe[1$], Glen McHale[1#], Sujung Ahn[2], Robert Bryant[2], Stefan H. Doerr[2] and Michael I. Newton[*]

[1]*School of Science and Technology, Nottingham Trent University, Clifton Lane, Nottingham, NG11 8NS, United Kingdom*

[2]*College of Science, Swansea University, Singleton Park, Swansea, SA2 8PP, United Kingdom*

Abstract

The wettability of soil is of great importance for plants and soil biota, and in determining the risk for preferential flow, surface runoff, flooding and soil erosion. The molarity of ethanol droplet (MED) test is widely used for quantifying the severity of water repellency in soils that show reduced wettability and is assumed to be independent of soil particle size. The minimum ethanol concentration at which droplet penetration occurs within a short time (≤ 10 s) provides an estimate of the initial advancing contact angle at which spontaneous wetting is expected. In this study, we test the assumption of particle size independence using a simple model of soil, represented by layers of small (~0.2 to 2 mm) diameter beads that predict the effect of changing bead radius in the top layer on capillary driven imbibition. Experimental results using a three-layer bead system show broad agreement with the model and demonstrate a dependence of the MED test on particle size. The results show that the critical initial advancing contact angle for penetration can be considerably less than 90° and varies with particle size, demonstrating that a key assumption currently used in the MED testing of soil is not necessarily valid.
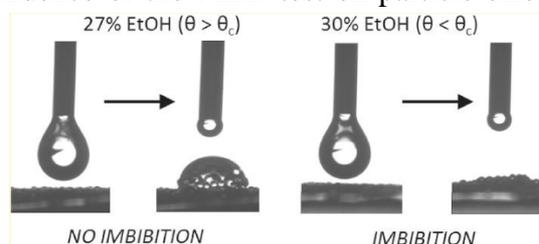
Keywords: Soil, MED, wetting, water repellent.

[*] To whom correspondence should be addressed. E-mail: michael.newton@ntu.ac.uk
[$]Now at Rhine-Waal University of Applied Science, Germany
[#]Now at University of Northumbria, UK

INTRODUCTION

The wettability of soil is of great importance for plants and soil biota, and in determining the risk for preferential flow, surface runoff, flooding and soil erosion.[1-3] There are a range of distinctive environmental conditions that can give rise to water repellent soil. It is well established that fires can volatilize hydrophobic compounds in the vegetation, litter or soil and these vapors can then condense on the sandy particles producing a hydrophobic granular texture that can exhibit high levels of water repellency. Under these circumstances vegetation recovery can be delayed, which further increases rates of surface runoff and erosion, and, on some slopes, the risk of debris flows.[4] Where land with naturally high levels of water repellency, such as eucalyptus forest, is cleared for farming, productivity can be affected. This can be alleviated, but only at significant cost to farmers, by mixing in substantial amounts of clay.[5] Where grey water is used for irrigation, or soil has been used as a natural filter for waste-water disposal, crop productivity can be significantly reduced due to the gradual increase in soil water repellency.[6] A less benign origin of soil or sediment water repellency is from hydrocarbon contamination. Such contaminated sites can show a long-term persistence in water repellency, which can sometimes re-establish itself after attempts to remediate the land.[7] In these types of situations it is important to be able to monitor and classify water repellency.

The Molarity of Ethanol Droplet (MED) test[1], which is sometimes referred to as the Critical Surface Tension[2] and %Ethanol[3] test is used widely to determine the severity of water repellency for soil and other porous or granular samples. It involves placing drops of aqueous ethanol solutions with decreasing surface tension on to different areas of the sample surface until a solution of sufficiently low surface tension is reached that just allows the drops to penetrate the soil within 3 to 10 seconds. The molarity (MED), concentration (%Ethanol) of the solution, or the surface tension allowing the porous surface to be penetrated by the liquid, is then taken as being characteristic for that soil. This method has been shown to be quite reproducible and diagnostic of soil water repellency, provided soil samples are reasonably dry, homogenized and atmospheric conditions are controlled.[3,8-10] The relationship between surface tension and the equilibrium contact angle, a concept that assumes there is contact angle hysteresis, is often described by Young's equation. In the MED test it is assumed reducing the surface tension causes imbibition by reducing this contact angle to below 90° at which point a parallel walled capillary would spontaneously fill. The surface tension of the solution that just penetrates the soil, γ_c (i.e. the critical surface tension for penetration), has been used to estimate the average surface energy of the soil.[2,11] It should be noted that the critical surface tension defined in this manner is not the same as the critical surface tension often referred to within surface science and typically obtained from a Zisman plot by extrapolating the results of contact angle measurements using a range of liquids to give an estimated surface tension at which a smooth flat surface would be completely wetted.[12,13] It has also been suggested[14] that the (initial advancing) contact angle at the surface tension, which gives wetting into water repellent soil or other granular materials, is not 90° as often assumed, but is closer to 51° when the dominating forces are capillary and a model of hexagonal close-packed spherical particles can be assumed. Experimental data suggested a contact angle of around 61°-65° could describe the critical surface tension for penetration into water repellent sand. Given that the initial advancing contact angle for penetration can be considerably less than 90° according to these reports, it is important to assess whether the MED test is independent of particle size and whether there are consequences for the implied initial advancing contact angle.

Here we extend this previous work by developing a model of the conditions under which a liquid will penetrate under capillary forces into a hexagonal symmetry pack of spherical particles (beads). This model uses a surface layer of beads that have a smaller radius than those upon which they rest, which themselves are in a close-packed arrangement. The model predicts that penetration will occur at a critical advancing contact angle for the liquid that depends on the ratio of the two sizes of beads. This implies that the advancing contact angle at the surface tension, which gives wetting into soil, can be above 51° when the surface layer of beads are smaller than subsequent layers. This implies that the MED test gives a critical advancing contact angle that is dependent on the arrangement of particles and their sizes. We then develop a systematic method of creating bead packs with the model geometry and use an MED test approach to assess the critical advancing contact angle at which ethanol solutions penetrate them. The experimental data is shown to follow the trend predicted by the model, but with penetration occurring at systematically lower concentrations corresponding to higher advancing contact angles. An implication of this work is that the MED test may give results that require subtle analysis to be able to classify the severity of water repellency for granular material such as soil.

GEOMETRIC MODEL

To examine the effect of particle size on capillary driven droplet infiltration into hydrophobic soil and granular systems sandy soil particles can be modeled using packs of spherical particles (beads). For the transition from a system in which water does not penetrate to one which it does, one can imagine the top (surface) layer composed of beads of a radius r laying on top of close-packed beads having a larger radius R, thereby introducing a loose-packing element to the surface layer arrangement (Figures 1a and 1b). This allows the separation between surface particles and the distance from the top of particles in the surface layer to the top of particles in the layer below to be altered whilst retaining a hexagonal symmetry of the top layer arrangement. This symmetry can be visualized by imagining a pyramid (tetrahedral) arrangement defined by a bead in the top layer resting on the space defined by three close-packed beads of the layer below (Fig. 1). The base-to-apex height of the pyramid can be found from the geometry of Fig. 1a,b.

$$p_h = \sqrt{(R+r)^2 - \frac{4R^2}{3}}$$

$$d_c = (p_h + r - R)$$

$$\cos\theta_c = \frac{d_c - r}{r} = \frac{p_h - R}{r}$$
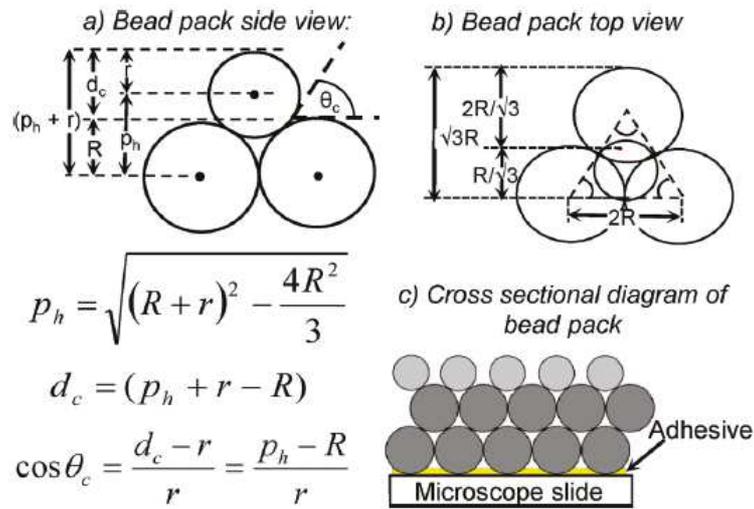
Figure 1. Schematic representations of bead packing of a surface layer on top of a layer of close packed beads (side view (a) and top view (b)), equations relating the relevant lengths and configuration of bead beds investigated by MED tests (c).

From consideration of the surface free energy, the condition for capillary driven imbibition of a liquid into the beads is when the wetting front of an impinging liquid, touches the beads in the layer below; should this happen the liquid will then continue into the subsequent layers giving full penetration of the bead pack. This condition is met when the wetting front has an equilibrium position at a critical distance (d_c) measured from the top of the beads in the top layer to the top of the beads in the layer below. Assuming that the liquid has a horizontal meniscus as it bridges between three adjacent beads defining a pore, this has an associated critical angle of contact (θ_c), at the liquid / solid / vapor phase boundary. The critical depth is determined by the comparative sizes of the beads in the top layer and subsequent layers of the bead pack provided only capillary forces are important and gravity can be ignored. From the geometry of Fig. 1, the model predicts,

$$\cos\theta_c = \frac{R}{r}\left[\sqrt{\left(1+\frac{r}{R}\right)^2 - \frac{4}{3}} - 1\right] \qquad (1)$$

For eq. (1) to be valid, capillary forces must dominate over gravity, and this requires the separations between beads to be significantly less than the capillary length of the liquid $\kappa^{-1}=(\gamma/\rho g)^{1/2}$, where γ is the surface tension of the liquid, ρ is its density and $g=9.81$ ms^{-2} is the acceleration due to gravity. In this model, any liquid with an advancing contact angle, θ_A, below that of the critical angle contact will penetrate into the bead pack. In the case of a uniform particle size throughout the particle bed (i.e. $r/R=1$) the predicted critical angle is 50.73°, which is consistent with previous work reported in the literature.[14,15]

EXPERIMENTAL METHODS

Glass beads of different sieve fractions in the size ranges 0.18-0.21 mm up to 1.8-2.0 mm (General Purpose Glass Microspheres, Whitehouse Scientific, a full list of sizes are included in the supplementary material), comparable to sizes found in sandy soils, were immersed in HCl (30 vol. %) for 24 hours and then rinsed with UHQ H$_2$O (resistivity = 18 MΩ.cm^{-1}) and dried for 4 hours at 110 °C. The hydrophilic glass beads were then immersed in chlorotrimethylsilane (CTMS) (2 vol.% in toluene; CTMS purchased from Aldrich) for 48 hours at room temperature then rinsed with toluene and allowed to air dry. CTMS was chosen because it provides a high contact angle to solutions of ethanol and persistent repellency on contact with the liquid, thereby being suitable for MED type experiments seeking to determine the initial advancing contact angle. Bead packs were constructed by placing the glass beads into a triangular template etched into laser-cut acrylic sheet and agitated until the beads formed a close packed monolayer (Fig. 1c). A layer (~110 μm thick) of polyurethane adhesive (1A33, Humiseal) was applied to a glass microscope slide, which was then placed on top of the beads, removed and a thin triangular acetate frame placed around the beads. The adhesive was then cured at 80 °C for 16 hours fixing this initial layer of beads in place and so providing a hexagonal packing symmetry for registration of subsequent layers of beads. A second acetate frame, with a slightly smaller triangular hole than the first, was then stuck to the first frame using double sided tape and a second layer of beads was poured into the frame and agitated until close packed. This layer of beads therefore registered with the first layer, but was loose and not fixed by any adhesive. This process was repeated for a third bead layer but this time using a frame of approximately half the bead thickness so the top of the third layer was exposed. This method of constructing a three-layer bead pack ensured a fixed base layer with a hexagonal close-packed structure acting as a template to ensure registration of subsequent layers of beads, which themselves

did not include adhesive bonding that might interact with a penetrating liquid in the experiments (Fig. 1). We also conducted tests with bead packs with more than three layers (top layer with beads of radius r and other layers with beads of radius R) and did not find any significant differences in the ethanol concentrations at which penetration began.

The surface tensions, γ_{etOH}, of ethanol solutions, for use in the MED tests, were measured using a Du Nouy ring at 25°C. The corresponding advancing contact angle, θ_A, on a CTMS treated flat glass microscope slide was measured using a Krüss DSA 10 contact angle meter by depositing a droplet of ethanol solution and increasing its volume to 20 µl at a rate of 20 µl.min^{-1}. The observed contact angle was measured using Krüss DSA software and the value just prior to the droplet's contact line moving was taken as the advancing contact angle. The surface tension of the ethanol solutions were consistent with those reported in the literature[16] and exhibit a range of advancing contact angles sufficient to investigate a range of r/R values of up to 1 (θ_c=50.73°)[14,15] (Figure 2).
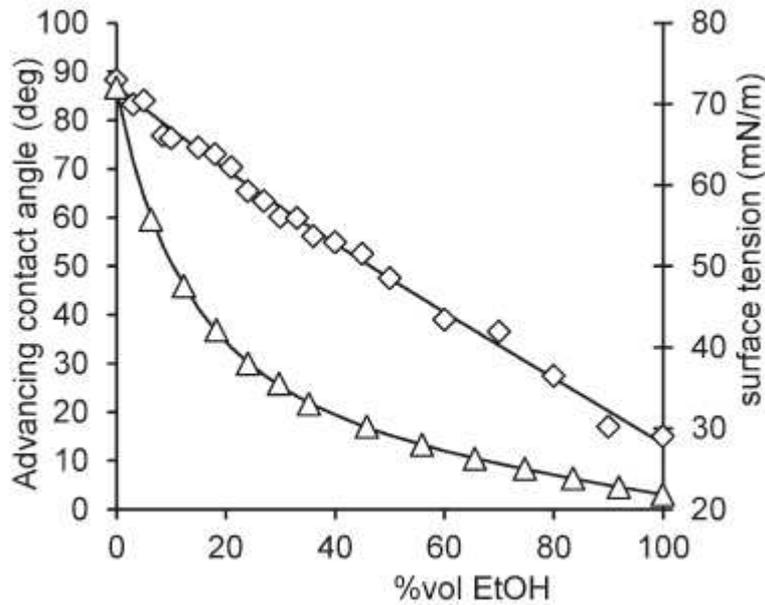
Figure 2. Advancing contact angle (measured on CTMS modified glass slides) and surface tensions of ethanol solutions in water used for MED tests (Literature values shown are taken from reference 12).

Since an MED test uses a range of concentrations of ethanol to estimate the advancing contact angle at which an ethanol solution just penetrates a porous system it is useful to be able to transform numerically from ethanol concentration, c, to surface tension or advancing contact angle (on CTMS modified glass surfaces). This can be achieved by creating interpolation equations through the data,

$$\theta_A(c) = -0.0000126c^3 + 0.0029998c^2 - 0.090953c + 87.022 \qquad (2)$$

and

$$\gamma_{EtOH}^{-1}(c) = -1.2804 \times 10^{-10}c^4 + 5.1594 \times 10^{-8}c^3 - 7.2619 \times 10^{-6}c^2 + 6.5721 \times 10^{-4}c + 1.3954 \times 10^{-2} \quad (3)$$

where c is the ethanol concentration by volume percentage, θ_A is the advancing contact angle in degrees and γ_{EtOH}^{-1} is the inverse surface tension in units of m mN^{-1}. The accuracy of these interpolation formulae compared to the data is shown in the supplementary information and the

surface tension interpolation predicts the data of Vasquez *et al.*[16] to within 0.5%. An important parameter for knowing whether capillary forces dominate over gravitational forces is the capillary length, κ^{-1}. In the MED test, both the surface tension and the density vary with ethanol concentration and so we also measured the changes in density and have constructed an interpolation formula for the (inverse) capillary length,

$$\kappa_{EtOH}(c) = -3.9315 \times 10^{-9} c^4 + 1.1489 \times 10^{-6} c^3 - 1.2949 \times 10^{-4} c^2 + 7.6214 \times 10^{-3} c + 0.37077 \quad (4)$$

where eq. (4) gives the inverse capillary length in units of mm^{-1}. Thus, for a 0% v/v concentration of ethanol (i.e. pure water), the capillary length is κ^{-1}=2.70 mm and as ethanol concentration increases the capillary length reduces, e.g, at 20% v/v ethanol the capillary length is κ^{-1}=2.08 mm.

MED tests were carried out by placing a single droplet (8 – 18 μl) of aqueous ethanol solution at various concentrations onto a bead pack with the use of a syringe controlled by a stepper motor. The imbibition time of the droplet into the bead pack was measured by the video system of the goniometer (frame rate of up to 25 fps). The drop volume depended on the concentration of EtOH in solution and a single droplet was used per MED test. To estimate the lowest concentration at which a solution penetrated within 10 seconds, we constructed a plot of imbibition time versus concentration of ethanol (see example MED curves in the supplementary information). Steps of 5% in concentration were used over the wider range and this was narrowed to steps of 3% around the concentrations at which a solution penetrated a bead pack. For each bead pack we observed a step-like transition curve in whether or not penetration occurred as the ethanol concentration was increased. The value of concentration at the transition to imbibition provides estimates of the initial advancing contact angle, $\theta_A{}^c$, and the surface tension, $\gamma_{etOH}{}^c$, for penetration *via* the interpolation eqs. (2) and (3). The plots together with the interpolation equations also allow the uncertainty of these values to be quantified. The measured value of $\theta_A{}^c$ can then be compared to the critical angle of contact, θ_c, from eq. (1) predicted by the model on the basis of the relative bead sizes.

RESULTS AND DISCUSSION

Figure 3 shows the measured threshold ethanol concentrations for penetration as a function of bead size for bead packs with $r/R = 1$ (i.e. top layer beads having the same diameter as the lower two layers) thereby investigating whether absolute bead size matters; the secondary *y*-axis shows the equivalent values of advancing contact angle $\theta_A{}^c$ as deduced from eq. (2). This tests whether or not the assumption that capillary forces are dominant is valid for the various bead sizes used to obtain r/R=1. As bead size reduces the capillary forces can be sufficiently strong that on contact with the lower surface of a droplet a bead is lifted up from the top layer of beads as the droplet surface is shaped by its surface tension. Bead lifting is caused by the strength of capillary forces relative to the force of gravity acting upon a loose bead and is related to the ability of droplets to encapsulate themselves with a shell of hydrophobic particles to create liquid marbles.[17,18] The data for the three-layer close packed beads are shown as solid circles where bead lifting was observed and as open circles where it was not. In these experiments we also constructed and tested penetration of ethanol solutions into much thicker randomly packed beds of CTMS treated glass-beads from single size sieve fractions of beads and these data points are shown as solid diamond symbols. From this figure we can see that the threshold ethanol concentration, and hence critical advancing contact angle $\theta_A{}^c$, increases as bead size increases. This is consistent with geometrical considerations for a hexagonal arrangement of spherical beads, which show that the radius of the

meniscus, r_{gap}, between three close-packed beads defining a pore at an angle of contact θ_c is $r_{gap}=0.866R(1-r\sin\theta_c/0.866R)$ so that the assumption $r_{gap}/\kappa^{-1}<<1$ needed for gravity to be ignored fails as the bead size increases. At larger bead sizes the results show some scatter with contact angles between 65° and 85° and this probably arises from small imperfections in the shape and monodispersity of the beads creating defects in the hexagonal symmetry of the packing and, hence, larger gaps through which imbibition can commence.
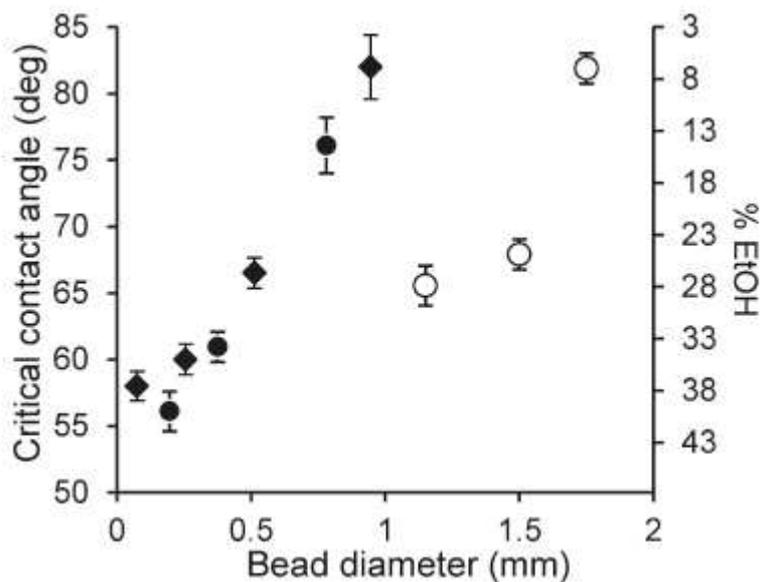
Figure 3. Ethanol concentration and advancing contact angles for penetration as determined by MED tests, of various 3 layer bead packs and loose packed beds with $r/R=1$. Solid circles show where bead lifting was observed and open circles where it was not observed. Solid diamond symbols show data from thick random loose-packed beds.
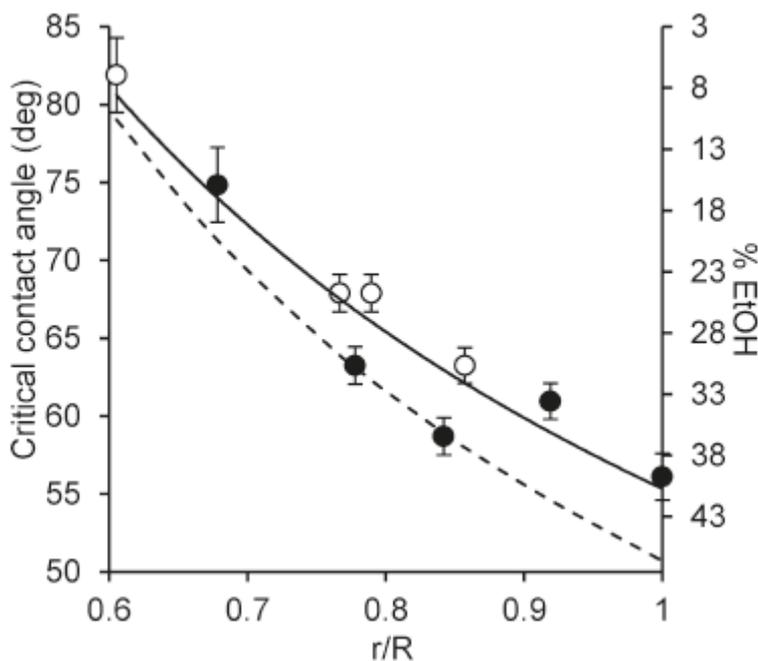
Figure 4. Ethanol concentration and advancing contact angles for penetration into three-layer bead packs of varying r/R as determined by MED tests. Solid circles show where bead lifting was observed and open circles where it was not observed. The dashed line shows the theoretical curve and the solid line the fit to the experimental points.

The results of the MED tests on close packed hydrophobic beads with a range of r/R values are shown in Figure 4 with a comparison to the theoretical model (dashed line) and fit to the data (solid line). Similar to fig. 3, eq. (2) has been used to present that data with two y-axes thereby allowing a simple comparison between the percentage of ethanol and the equivalent advancing contact angle at which penetration occurs. This data contains data from two types of bead packs constructed using, i) only mono-disperse beads and ii) beads of sieved ranges (open circles where the beads showed no lifting and solid circles where bead lifting was observed). Details of the sieved ranges can be found in the supplementary material. The trend of the data follows that of the theoretical curve with the value of the critical advancing contact angle $\theta_A{}^c$, decreasing significantly below 90° as the r/R ratio increases towards unity although the data tends to lie slightly above the theoretical curve. This may result from any defects in bead packing associated with variation in shape and/or size of adjacent beads within the packs producing defects and larger gaps between beads compared with model predictions and capillary length.

The approach in this work uses a hexagonal symmetry packing model with hydrophobic spherical beads and is valid only under conditions where capillary forces are dominant. It does, however, provide a test of the prediction that under these conditions complete penetration occurs when the meniscus of the liquid advancing down the loose-packed surface layer comes into contact with particles from the layer below. This is a general principle for capillary driven penetration that should be applicable to other types of packing and to non-spherical particles. Should pores in the system approach in size to the capillary length or large defects with substantial pore size be present, penetration will occur at much lower ethanol concentrations. Similarly, the model does not include effects of a hydrostatic pressure. The model is intended to improve understanding of the MED test, which itself provides an estimate only of the initial advancing contact angle. In any system where the hydrophobicity of the particle coating changes over time on contact with water, the test will not provide an accurate indication of the length of time over which soil will remain repellent as indicated in previous work empirically[8] and by direct observation of soil particle coatings.[19] Similarly, prolonged exposure will lead to adsorbed vapors on particles and this may itself cause changes to the contact angle and hence lead to penetration of water.

This work shows that the critical initial advancing contact angle for penetration into particle beds taken to represent sandy soil can be considerably less than $90°$ and varies with particle size. If soils of different particle size distributions are compared, the critical initial advancing contact angle $\theta_A{}^c$ is likely to vary although some trends with both absolute size and packing of the layers can be expected. The results demonstrate that the widely held assumption[11] that a liquid will just enter a porous substrate when it has a contact angle of $90°$ is not necessarily valid. This has important implications for evaluating the wettability of soils and other granular materials. Some soils or granular materials previously classified as fully wettable, based on MED, surface tension or %Ethanol tests, may, in fact, exhibit a significant resistance to wetting, which in turn bear some of the environmental implications typically associated with the presence of water repellency.

ACKNOWLEDGMENT

SUPPORTING INFORMATION AVAILABLE

The contents of Supporting Information includes the following: (1) table showing bead size and source (2) example graph of MED data (3) graph of data and interpolation for advancing contact angle as a function of ethanol concentration, (4) graph of data and interpolation for 1/surface tension as a function of ethanol concentration (5) graph of data and interpolation for 1/ capillary length as a function of ethanol concentration. This information is available free of charge via the Internet at http://pubs.acs.org/.

REFERENCES

1   King, P. M. Comparison of methods for measuring severity of water repellence of sandy soils and assessment of some factors that affect its measurement. *Aust. J. Soil Res.* **1981**, *19* (4), 275-285.

2   Watson, C. L.; Letey, J. Indices for characterizing soil-water repellency based upon contact angle-surface tension relationships. *Soil Sci. Soc. Am. J.* **1970**, *34* (6), 841-844.

3   Dekker, L. W.; Ritsema, C. J. How water moves in a water repellent sandy soil. 1. potential and actual water repellency. *Water Resour. Res.* **1994**, *30* (9), 2507-2517.

4   DeBano, L. F. The role of fire and soil heating on water repellency in wildland environments: A review. *J. Hydrol.* **2000**, *231*, 195-206.

5   Cann, M. A. Clay spreading on water repellent sands in the South East of South Australia-Promoting sustainable agriculture. *J. Hydrol.* **2000**, *231*, 333-341.

6   Mataix-Solera, J.; García-Irles, L.; Morugán, A.; Doerr, S.H.; Garcia-Orenes, F.; Arcenegui, V.; Atanassova, I. Longevity of soil water repellency in a former wastewater disposal tree stand and potential amelioration. *Geoderma* **2011**, *165* (1), 78-83.

7   Roy, J. L.; McGill, W. B. Investigation into mechanisms leading to the development, spread and persistence of soil water repellency following contamination by crude oil. *Can. J. Soil Sci.* **2000**, *80* (4), 595-606.

8   Doerr, S. H. On standardizing the 'water drop penetration time' and the 'molarity of an ethanol droplet' techniques to classify soil hydrophobicity: A case study using medium textured soils. *Earth Surf. Proc. Landforms.* **1998**, *23* (7), 663-668.

9   Doerr, S. H.; Dekker, L.; W. Ritsema, C. J.; Shakesby R. A.; Bryant. R. Water repellency of soils: The influence of ambient relative. *Soil Sci. Soc. Am. J.* **2002**, *66* (2), 401-405.

10   Roy, J. L.; McGill, W. B. Assessing soil water repellency using the molarity of ethanol droplet (MED) test. *Soil Sci.* **2002**, *167* (2), 83-97.

11   Letey, J.; Carrillo, M. L. K.; Pang, X. P. Approaches to characterize the degree of water repellency. *J. Hydrol.* **2000**, 231, 61-65.

12   Zisman, W. A. 1964. Relation of equilibrium contact angle to liquid and solid constitution. In Contact Angle Wettability and Adhesion. Advances in Chemistry Series, Vol. 43. R.F. Gould (ed.). American Chemical Society, Washington, DC, pp. 1–51.

13   Adamson, A. W. & Gast, A. Physical Chemistry of Surfaces (Wiley-Blackwell, 1997).

14   Shirtcliffe, N. J.; McHale, G.; Newton M. I.; Pyatt, F. B. Critical conditions for the wetting of soils. *Appl. Phys. Lett.* **2006**, *89* (9), 094101.

15   Bán, S.; Wolfram, E.; Rohrsetzer, S. The condition of starting of liquid imbibition in powders. *Colloids Surf.* **1987**, *22* (2-4) 301-309.

16   Vázquez, G.; Alvarez, E.; Navaza, J. M. Surface tension of alcohol plus water from 20 degrees C to 50 degrees C. **1995**, *40* (3) 611-614.

17   McHale, G.; Shirtcliffe, N.,J.; Newton, M.,I.; Pyatt, F.,B.; Doerr, S. H. Self-organization of hydrophobic soil and granular surfaces. *Appl. Phys. Lett.* **2007**, *90* (5), 054110.

18   McHale, G.; Newton, M.,I. Liquid marbles: principles and applications. *Soft Matter* **2011**, *7* (12) 5473-5481.

19   Cheng, S.; Bryant, R.; Doerr, S. H.; Wright, C. J.; Williams, R. Investigation of Surface Properties of Soil Particles and Model Materials with Contrasting Hydrophobicity Using Atomic Force Microscopy. *Environ. Sci. Technol.* **2009**, 43 (17), 6500–6506.

Table S1. Table of glass beads of different sieve fractions in the size ranges 0.18-0.21 mm up to 1.8-2.0 mm used in the work.

Sieve range of beads in bottom layer / mm *(Catalogue number from Whitehouse Scientific)*	Radius of beads in bottom layer (R) / mm	Sieve range of beads in top layer / mm *(Catalogue number from Whitehouse Scientific)*	Radius of beads in top layer (r) / mm	r/R
0.18 – 0.212 *(GP0196)*	0.098	0.18 – 0.212 *(GP0196)*	0.098	1.00
0.35 – 0.40 *(GP0375)*	0.1875	0.35 – 0.40 *(GP0375)*	0.1875	1.00
0.710 – 0.85 *(GP0780)*	0.39	0.71 – 0.85 *(GP0780)*	0.39	1.00
1.12 – 1.18 *(GP1150)*	0.575	1.12 – 1.18 *(GP1150)*	0.575	1.00
1.40 – 1.60 *(GP1500)*	0.75	1.40 – 1.60 *(GP1500)*	0.75	1.00
1.70 – 1.80 *(GP1750)*	0.875	1.70 – 1.80 *(GP1750)*	0.875	1.00
0.1926 (monodisperse) *(MS0192)*	0.0963	0.177 (monodisperse) *(MS0177)*	0.0885	0.92
1.70 – 1.80 *(GP1750)*	0.875	1.40 - 1.60 *(GP1500)*	0.75	0.86
0.18 – 0.212 *(GP0196)*	0.098	0.15 – 0.18 *(GP0165)*	0.0825	0.84
1.80- 2.0 *(GP1900)*	0.95	1.40 – 1.60 *(GP1500)*	0.75	0.79
0.18 – 0.212 *(GP0196)*	0.098	0.125 – 0.150 *(GP0138)*	0.07	0.78
1.40 – 1.60 *(GP1500)*	0.75	1.12 – 1.18 *(GP1150)*	0.575	0.78
0.2009 (monodisperse) *(MS0201)*	0.10045	0.1558 (monodisperse) *(MS0516)*	0.0779	0.77
1.12 – 1.18 *(GP1150)*	0.575	0.71 – 0.85 *(GP0780)*	0.39	0.68
1.8 – 2.0 *(GP1900)*	0.95	1.12 – 1.18 *(GP1150)*	0.575	0.61

Example MED curves
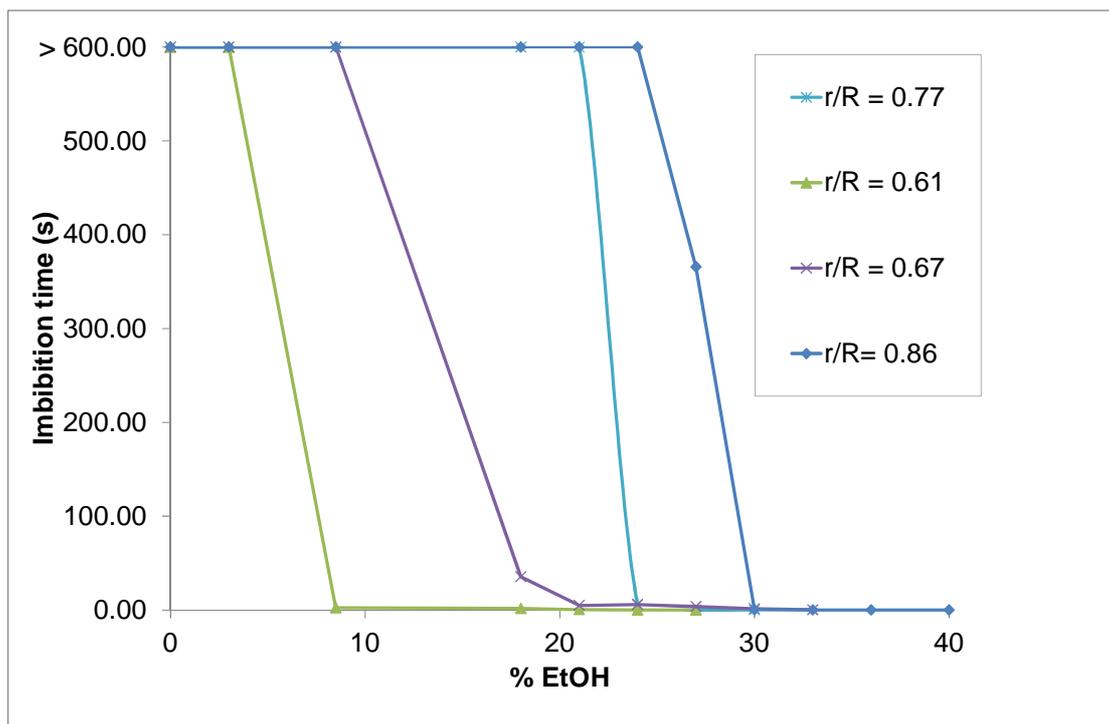
Figure S1. Typical examples of Molarity of Ethanol Droplet (MED) curves.
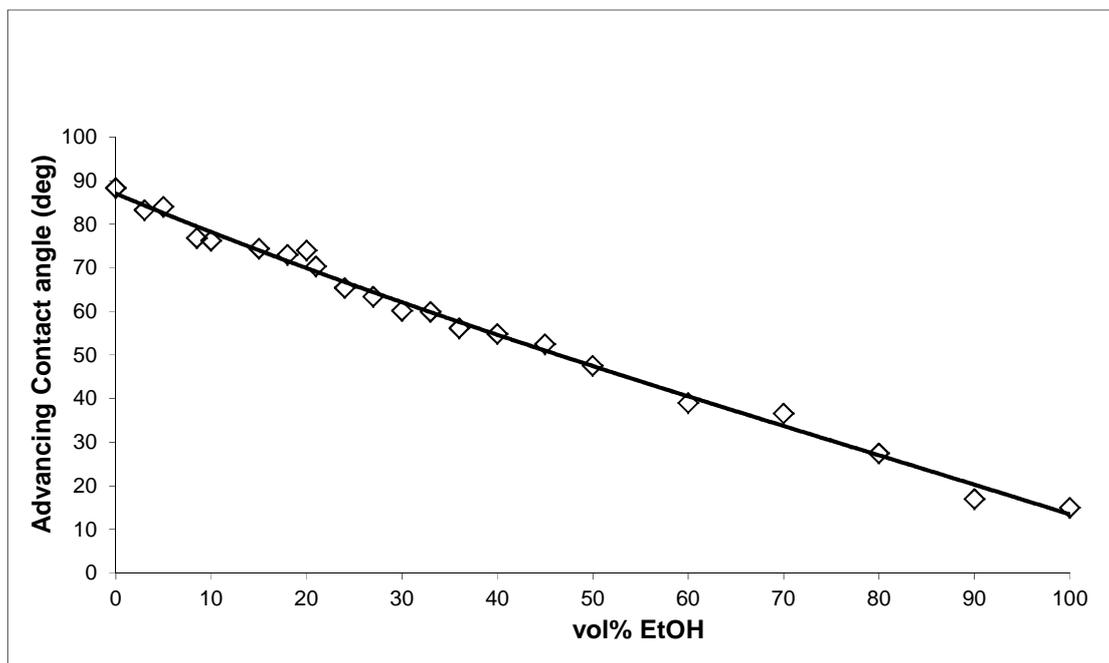
Figure S2. The solid line shows the interpolation to advancing contact angle for any concentration solution using equation 2 in the manuscript.
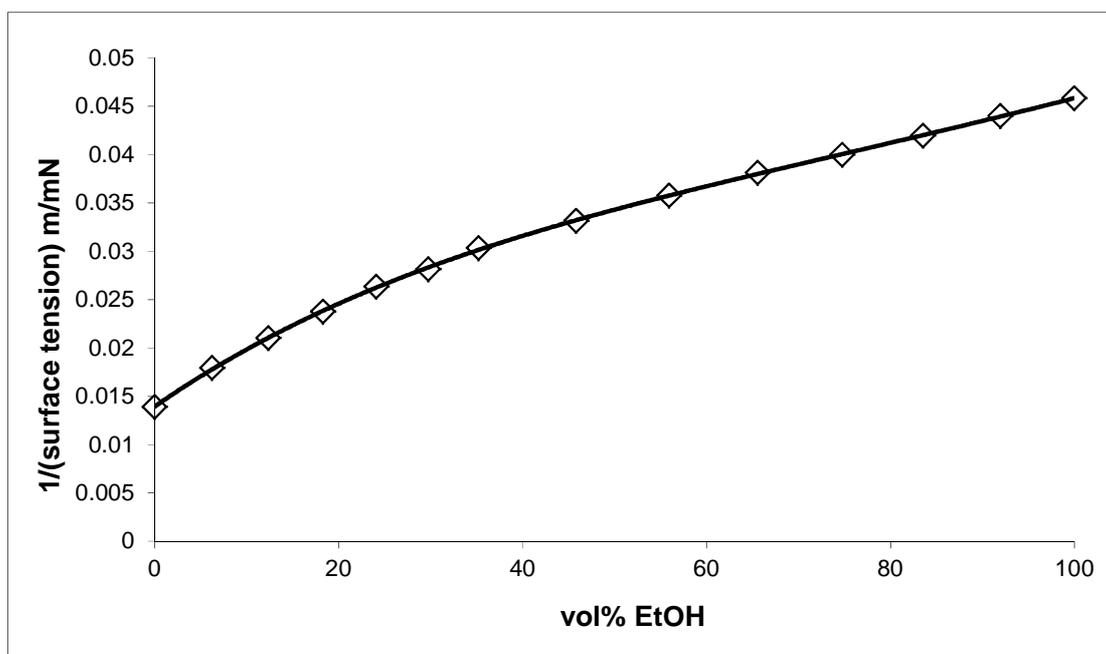
Figure S3. The solid line shows the interpolation to 1/surface tension for any concentration solution using equation 3 presented in the manuscript. Surface tensions of ethanol solutions in water literature values shown are taken from G. Vázquez, E. Alvarez and J. M. Navaza J.Chem. Eng. Data 40, 611 (1995).
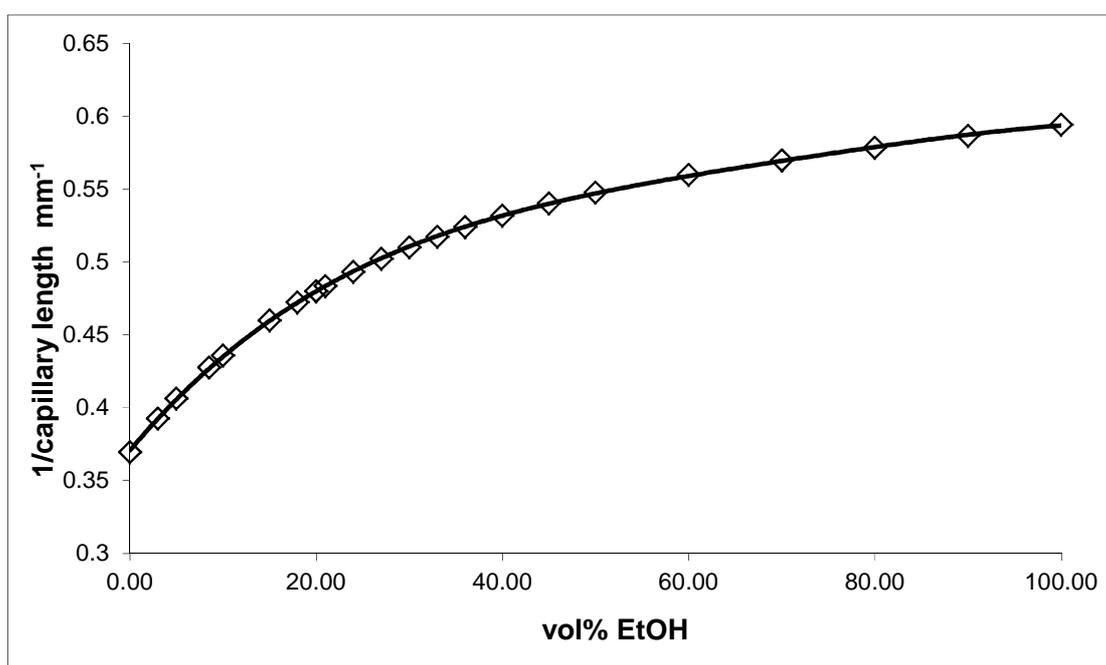
Figure S4. The solid line shows the interpolation to 1/ capillary length for any concentration solution using equation 4 presented in the manuscript.